

## **Tough Polycyclooctene Nanoporous Membranes from Etchable Block Copolymers (Supporting Information)**

Brenden D. Hoehn,<sup>†</sup> Elizabeth A. Kellstedt,<sup>§</sup> and Marc A. Hillmyer<sup>§,\*</sup>

<sup>†</sup>Department of Chemical Engineering and Materials Science, University of Minnesota,  
Minneapolis, MN 55455-0431

<sup>§</sup>Department of Chemistry, University of Minnesota, Minneapolis, MN 55455-0431

\*Corresponding author (e-mail: hillmyer@umn.edu)

### **Table of Contents**

Materials.....	S2
Characterization .....	S3–S5
Synthesis .....	S6–S7
Supplementary Figures and Tables .....	S8–S21
<sup>1</sup> H NMR spectra .....	S8–S9
IR spectra .....	S10–S12
DSC traces.....	S13
WAXS of triblock .....	S14
Photographs/SEM images of melt pressed and solvent cast films.....	S15
Tensile testing statistics (table) .....	S16
SEM micrographs of plasma treated membranes.....	S17–18
Water flux apparatus .....	S19
Gas flux apparatus.....	S20
References .....	S21

## *Materials*

*Cis*-cyclooctene (Sigma-Aldrich, 95%), 2-methyltetrahydrofuran (Sigma-Aldrich,  $\geq 99.0\%$ ), and tin(II) 2-ethylhexanoate ( $\text{Sn}(\text{Oct})_2$ , Sigma-Aldrich,  $\geq 92.5\%$ ) were distilled prior to use. Dry toluene (Sigma-Aldrich, 99%) was dispensed from an MBraun solvent drying system. D,L-lactide (Sigma-Aldrich, 95%) was recrystallized from ethyl acetate (Sigma-Aldrich, 99%) and toluene then stored in a glove box. Grubbs 2<sup>nd</sup> generation catalyst (Sigma-Aldrich), *cis*-ambrettolide (Perfumer Supply House), ethyl vinyl ether (Sigma-Aldrich, 99%), lithium aluminum hydride (Sigma-Aldrich,  $\geq 95.0\%$ ), sodium hydroxide pellets (Fisher Scientific), butylated hydroxytoluene (BHT, Sigma-Aldrich, 99%), chloroform (Sigma-Aldrich, 99%), methanol (Sigma-Aldrich, 99%), tetrahydrofuran (THF, Sigma-Aldrich, 99%), and ethyl acetate (Sigma-Aldrich, 99%) were used as received. Polyethersulfone (0.03  $\mu\text{m}$  pore), nylon (0.1  $\mu\text{m}$  pore), and polycarbonate (0.1  $\mu\text{m}$  pore) membrane filters were purchased (Sterlitech Corporation); tensile bars were cut from membranes as received.

## Characterization

Nuclear magnetic resonance (NMR) was performed on either an AX-400 Bruker Avance III HD 400 MHz or HD-500 Bruker Avance III HD 500 MHz spectrometer. Samples were dissolved in  $\text{CDCl}_3$  and run at 298 Kelvin with relaxation delays between 10–12 seconds. Chemical shifts reported are relative to residual solvent peaks. Fourier-transform infrared (FT-IR) spectroscopy was performed using a Bruker Alpha-P ATR FT-IR spectrometer (Figure S4) and a Thermofisher Nicolett iS50 FTIR ATR spectrometer (Figures S5–S6) equipped with diamond crystals. Data was averaged over 64 scans collected using transmittance mode.

Size exclusion chromatography (SEC) measurements were performed using an Agilent Infinity 1260 series HPLC system, using THF as the eluent at 25 °C with a 1 mL  $\text{min}^{-1}$  flow rate. The instrument was equipped with a Styragel HR column, a HELEOS II (Wyatt Technology) multi-angle light scattering detector, and an Optilab T-rEX refractive index detector (Wyatt Technology). Samples were prepared by dissolving 3-5 mg polymer sample in THF, then passing it through a 0.2  $\mu\text{m}$  syringe filter. Weight average molar masses ( $M_w$ ) were determined using light scattering and dispersities ( $D$ ) were determined using differential refractive index. The  $\text{dn/dc}$  value used for PCOE was 0.111  $\text{mL g}^{-1}$ , as previously reported; the  $\text{dn/dc}$  values of LCL triblock copolymers were a mass weighted average between PCOE and PLA (0.042  $\text{mL g}^{-1}$ ), typically 0.074–0.081  $\text{mL g}^{-1}$ .<sup>1,2,3</sup>

Differential scanning calorimetry (DSC) was used to analyze PCOE and LCL polymer samples using a Discovery Series DSC 2500 (TA Instruments) differential scanning calorimeter. 2–8 mg of dried polymer sample were placed in Tzero aluminum pans that were hermetically sealed under air. Samples were heated to 120 °C, cooled down to -85 °C, and heated once more to

120 °C. The heating/cooling rate was 10 °C min<sup>-1</sup>. Data was analyzed using Trios Software provided by TA Instruments.

Small-angle X-ray scattering (SAXS) was performed at the DuPont-Northwestern-Dow Collaborative Access Team (DND-CAT) research center 5-ID-D beamline of the Advanced Photon Source at Argonne National Laboratory. Polymer films/membranes were placed in Tzero aluminum pans and hermetically sealed under nitrogen atmosphere. The variable temperature analysis consisted of heating the sample from 25 °C to 80 °C, annealing for 20 minutes, then cooling to 60 °C, cooling to 40 °C annealing for 30 minutes, and lastly cooling to 25 °C.

Scanning electron microscopy (SEM) was performed on etched membranes using a Hitachi SU8230 Field Emission Gun under high vacuum with acceleration voltage of 5 kV and current of 5 µA detecting secondary scattered electrons. All samples were sputter coated with 2 nm of platinum to avoid charge buildup using an ACE600 Sputter Coater.

Tensile testing was performed Shimadzu AGS-X 500N tensile tester with the accompanying Trapezium software. A constant strain rate of 5 mm min<sup>-1</sup> was used for all samples. Water contact angle measurements were made by mounting samples on a glass slide and analyzing them with a microscopic contact angle meter (Kyowa Interface Science Co) which used a pneumatic dispensing system. The capillary is first soaked in a water repelling agent then loaded with deionized water. The inner diameter of the capillary was 30 µm and produced droplets that were 100 µL in volume. The images were captured by a horizontal camera with a high magnification lens; these images were processed using FAMAS image processing software.

Membranes were prepared for water flux measurements by prewetting membranes with methanol and transferring the membrane to a beaker of deionized water. Water flux measurements were performed by placing membranes in a cross-flow system with a flow rate of 300 mL min<sup>-1</sup>

at pressure of 0.07 bar (10 psig). Permeate mass was monitored using a balance, and the permeate volume was determined assuming the density of water was 1 g mL<sup>-1</sup>. Gas flux measurements were performed by passing air through dry membranes at a pressure of 0.28 bar (4 psig). The volume of permeate gas was determined by measuring the volume of water displaced. Both water and air flux apparatuses are shown in Figures S13–S14.

## Synthesis

*Cis*-hexadec-7-ene-1,16-diol (C<sub>16</sub>-diol) was synthesized by reducing  $\omega$ -7-hexadecenolactone (ambrettolide) using lithium aluminum hydride (LAH) with methods previously reported.<sup>4,5</sup> Briefly, a 250 mL 3-neck round bottom flask with a magnetic stir bar was purged with argon for 30 minutes. Ambrettolide (5 mL, 18.9 mmol) and dry THF (60 mL, 739 mmol) were added to the flask via syringe. The solution was cooled to 0 °C using in an ice bath while stirring under argon. LAH (1.44 g, 37.9 mmol) was added in small portions (approximately 250 mg each); subsequent LAH additions were added only after the solution bubbling subsided. After all LAH was added, the solution stirred an additional 20 hours at room temperature. The solution was placed in an ice bath and deionized water (2 mL, 111 mmol) was slowly added to neutralize unreacted LAH. The salts were filtered, and the product was extracted into ethyl acetate, dried over magnesium sulfate, filtered, and concentrated *in vacuo* at 60 °C, yielding a white crystalline solid (3.3 g, 65% yield). <sup>1</sup>H NMR (500 MHz, CDCl<sub>3</sub>)  $\delta$  5.42–5.33 (m, 2H, –CH=CH–), 3.66 (t, 4H, –CH<sub>2</sub>–OH), 2.10–1.96 (m, 4H, –CH<sub>2</sub>–CH=), 1.64–1.54 (m, 4H, –CH<sub>2</sub>–CH<sub>2</sub>OH), 1.43–1.26 (m, 6H, –CH<sub>2</sub>–CH<sub>2</sub>–CH<sub>2</sub>–).

The hydroxy telechelic polycyclooctene (PCOE) synthesis is detailed in the main text. After terminating the reaction, an aliquot was taken to determine monomer conversion, then the polymer was purified by precipitating it twice into cold methanol containing BHT and dried at 40 °C *in vacuo*. <sup>1</sup>H NMR (500 MHz, CDCl<sub>3</sub>)  $\delta$  5.62–5.12 (m, 2H·n, –CH=CH–), 3.64 (q, 4H, –CH<sub>2</sub>–OH), 2.17–1.76 (m, 4H·n, –CH<sub>2</sub>–CH=), 1.50–1.08 (m, 8H·n, –CH<sub>2</sub>–CH<sub>2</sub>–CH<sub>2</sub>–), where n is the degree of polymerization.

A standard synthesis of poly(lactide-*block*-polycyclooctene-*block*-poly(lactide (PLA-*b*-PCOE-*b*-PLA, abbreviated LCL) triblock copolymer was performed by drying a magnetic stir bar,

glass pressure vessel, PTFE screw cap, and O-ring in a 120 °C drying oven and PCOE in a vacuum oven at 40 °C overnight. Then these contents are quickly transferred to a glove box where D,L-lactide, dry toluene, and Sn(Oct)<sub>2</sub> are stored. Additional experimental details are listed in the main text. <sup>1</sup>H NMR (500 MHz, CDCl<sub>3</sub>) δ 5.62–5.12 (m, 2H·n, –CH=CH–), 5.26–4.94 (m, 1H·m, –O–CH–C=O), 4.40–4.32 (m, 1H·m, HO–CH–C=O), 4.16–4.08 (m, 4H, –CH<sub>2</sub>–O–), 2.17–1.76 (m, 4H·n, –CH<sub>2</sub>–CH=), 1.67–1.46 (m, 3H·m, –CH–CH<sub>3</sub>), 1.50–1.08 (m, 8H·n, –CH<sub>2</sub>–CH<sub>2</sub>–CH<sub>2</sub>–), where n and m are the degree of polymerization for PCOE and PLA respectively.

Supplementary Figures and Tables

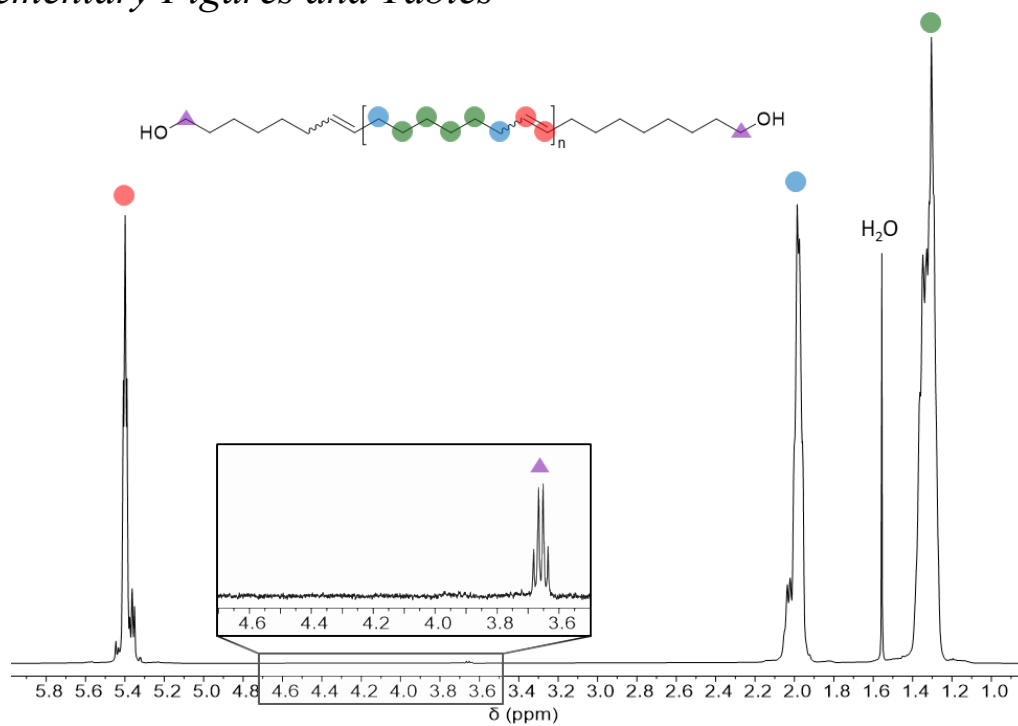


**Figure S1.** <sup>1</sup>H NMR spectrum of hydroxy telechelic PCOE PCOE [49] in CDCl<sub>3</sub>, 298 K.

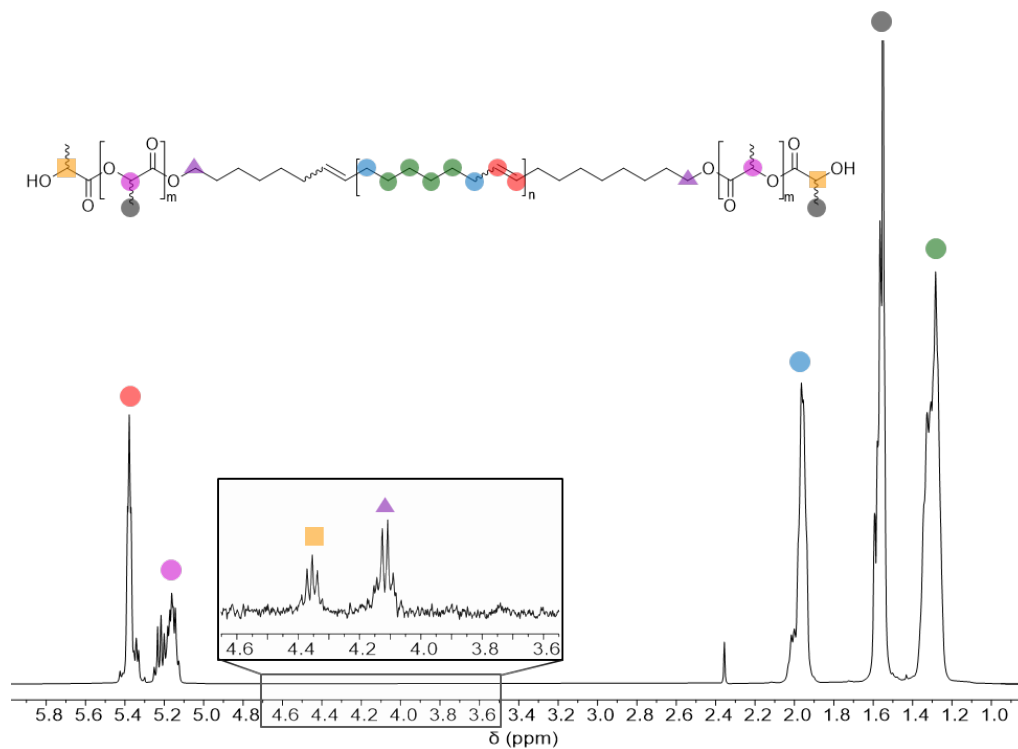


**Figure S2.** <sup>1</sup>H NMR spectrum of LCL [25-49-25] triblock copolymer in CDCl<sub>3</sub>, 298 K.



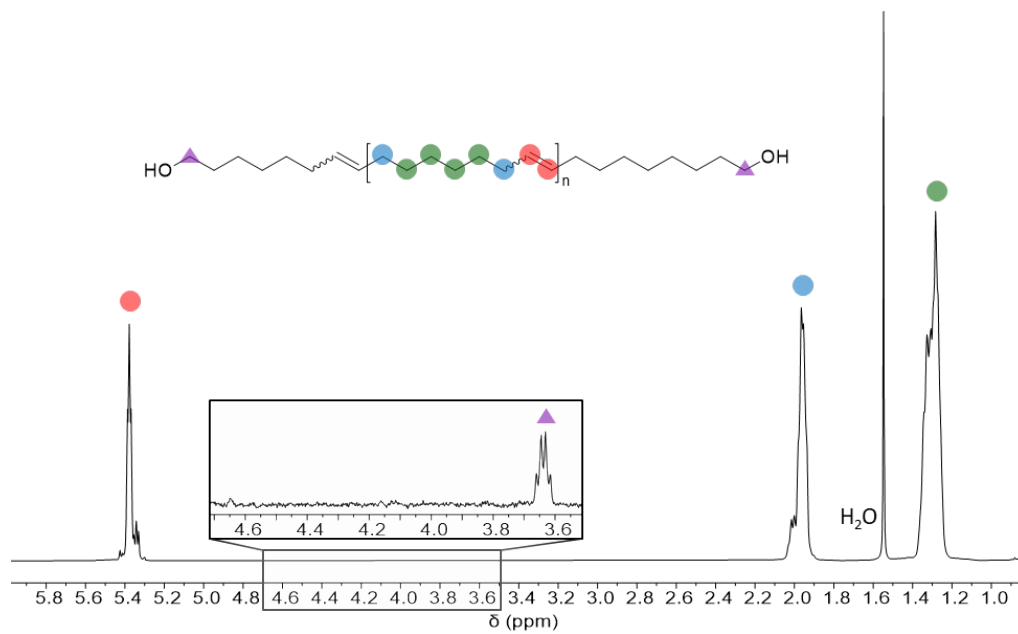


**Figure S3.** <sup>1</sup>H NMR spectrum of LCL [25-49-25] triblock copolymer (in CDCl<sub>3</sub>, 298 K) after PLA removal.

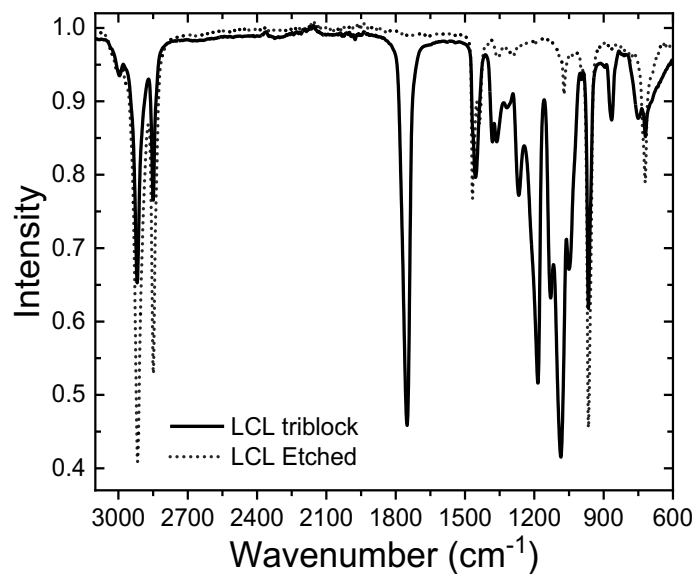


**Figure S4.** FT-IR spectra of LCL [26-50-26] and respective etched membrane.

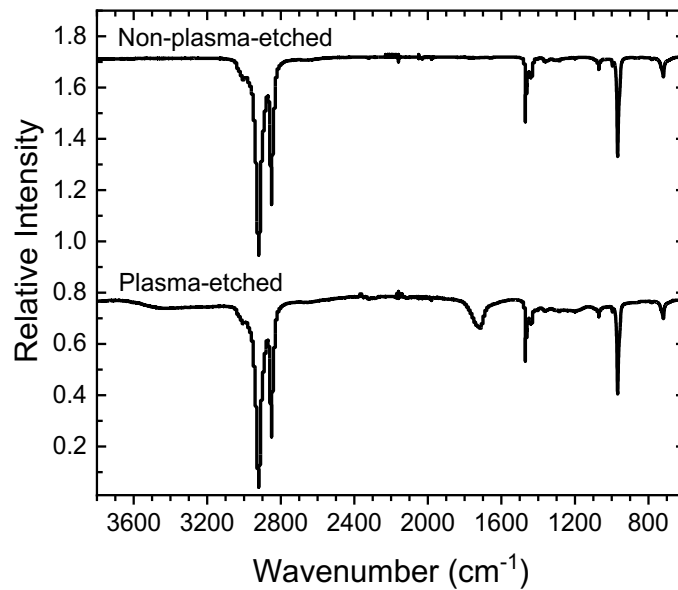


**Figure S5.** FT-IR spectra of nanoporous PCOE before and after etching. Non-plasma-etched membrane contains alkane (sharp peaks at: 2920, 2840, and 1470 cm<sup>-1</sup>) and alkene functional groups (sharp peak, 965 cm<sup>-1</sup>). In addition to these groups, the plasma-etched membrane shows hydroxyl (broad peak, 3400 cm<sup>-1</sup>) and carbonyl (medium peak, 1710 cm<sup>-1</sup>) groups on the surface.<sup>6,7</sup>

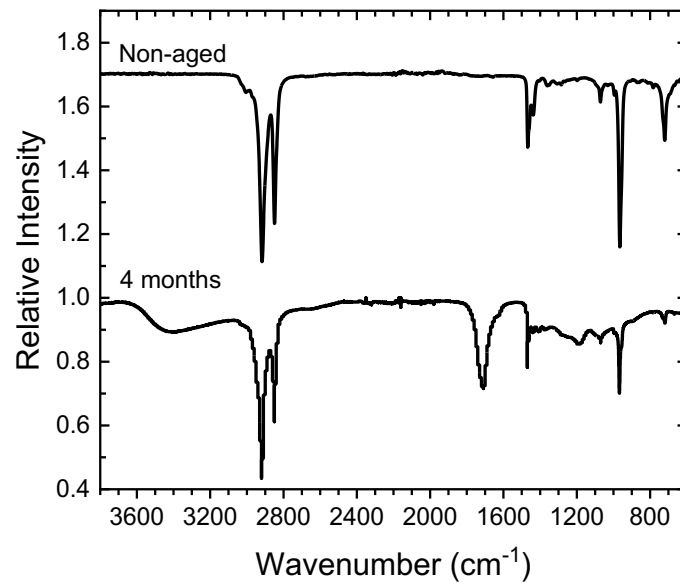


**Figure S6.** FT-IR spectra of nanoporous, PCOE samples directly following fabrication (non-aged) and after four months of aging under air, where signs of oxidation were evident in the aged sample.

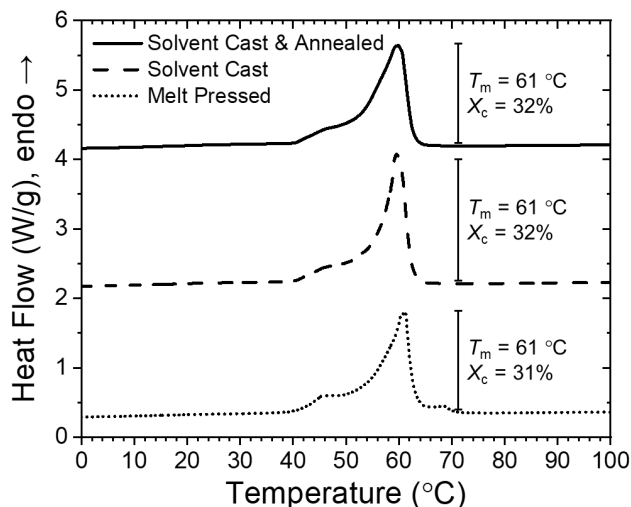


**Figure S7.** DSC traces for membranes derived from LCL [25-51-25] after varying film processing conditions. Data shown for 1<sup>st</sup> heating cycle. Crystallinity is calculated by normalizing the area under the curve melting peak by 230 J g<sup>-1</sup> for 100% crystalline PCOE. Peaks sifted for clarity.

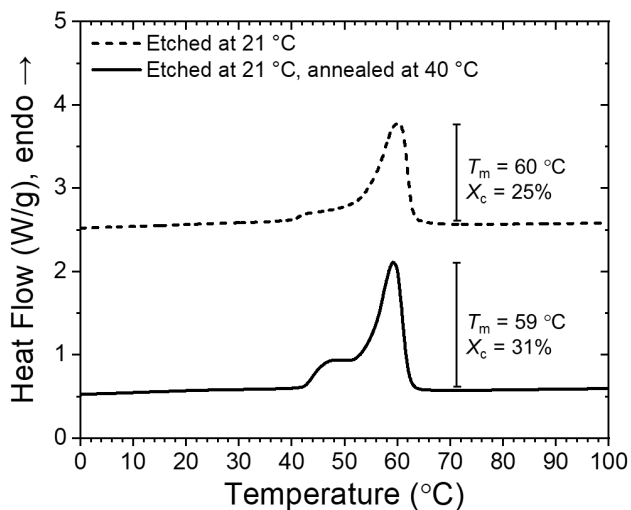


**Figure S8.** DSC traces for membranes derived from LCL [25-51-25] after etching at 21 °C for 24 hours. The bottom trace was then held isothermally at 40 °C for 3 hours. LCL films were solvent cast and annealed at 70 °C for 20 minutes prior to etching. Data shown for 1<sup>st</sup> heating cycle. Peaks sifted for clarity.

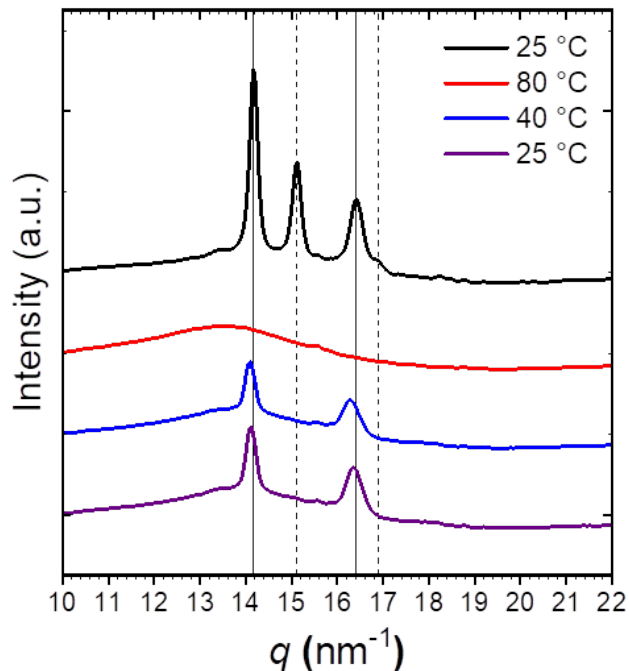


**Figure S9.** Variable temperature wide angle X-ray scattering (WAXS) analysis of LCL triblock copolymer. Curves correspond to 25 °C (black) as cast, 80 °C (red), 40 °C (blue), and 25 °C (purple) after thermal treatment. Samples were held isothermally at 80 °C for 20 minutes and 40 °C for 30 minutes. Shifted vertically for clarity. The black trace (triblock as solvent cast displays both a triclinic and monoclinic crystal structure. Heating the sample above the melting temperature melts all crystals. Cooling from the melt results in triclinic PCOE crystals. Triclinic crystal structure: peaks at  $14.2 \text{ nm}^{-1}$  and  $16.4 \text{ nm}^{-1}$  (solid lines) are characteristic of (010) and (110/-110) planes, space group:  $P-1$ .<sup>8</sup> Monoclinic crystal structure: peaks at  $15.1 \text{ nm}^{-1}$  and  $16.8 \text{ nm}^{-1}$  (dashed lines) are characteristic of (-110) and (200) planes, space group:  $P2_1/a$ .<sup>9</sup>

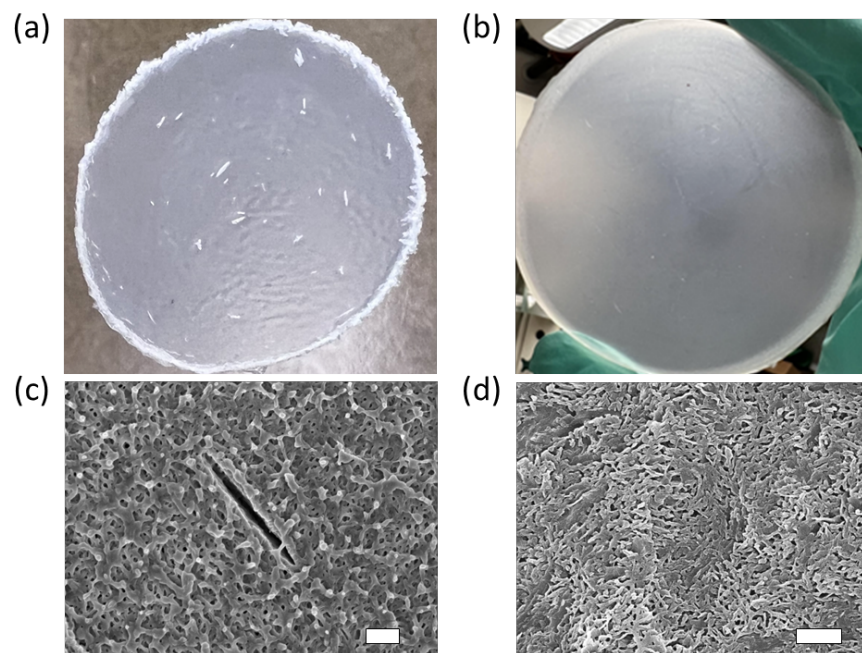


**Figure S10.** Photographs of (a) melt pressed and (b) solvent cast LCL films. SEM images of (c) melt pressed and (d) solvent cast NPMs. Crack dimensions in (c) are 4.6  $\mu\text{m}$  long and 300 nm wide. Scale bars representing 600 nm.

Processing History	Triblock or Membrane	Elastic Modulus (MPa)	Strain at break (%)	Ultimate tensile stress (MPa)	Toughness (MJ m <sup>-3</sup> )
Melt Pressed	Triblock	441 ± 60	213 ± 108	20.0 ± 6.6	36 ± 19
	Membrane	0.6 ± 0.1	12 ± 9	3.1 ± 1.5	0.3 ± 0.4
Solvent Cast	Triblock	526 ± 42	557 ± 59	27.7 ± 3.4	101 ± 14
	Membrane	70 ± 3	592 ± 69	8.6 ± 1.0	35 ± 5
Solvent Cast, Plasma etched	Membrane	118 ± 6	525 ± 68	8.2 ± 0.9	31 ± 6

**Table S1:** Tensile testing of LCL [25-51-25] films and membranes fabricated by melt pressing and solvent casting, and plasma etched membranes are also shown. Tabulated data shows a mean ± standard deviation for n > 5 samples.

Membrane Type	Elastic Modulus (MPa)	Strain at break (%)	Ultimate tensile stress (MPa)	Toughness (MJ m <sup>-3</sup> )
Polyethersulfone	108 ± 40	7 ± 1	2.6 ± 0.9	0.13 ± 0.06
Nylon	419 ± 70	33 ± 6	12.5 ± 2.8	4.2 ± 1.1
Polycarbonate	355 ± 73	25 ± 14	7.5 ± 1.9	1.8 ± 1.4

**Table S2.** Tensile testing of commercially available nanoporous membranes. Tensile samples were cut from as received membranes. Polyethersulfone and nylon membranes were fabricated using NIPS and polycarbonate membranes were fabricated via track etching. Tabulated data shows a mean ± standard deviation for n > 5 samples.



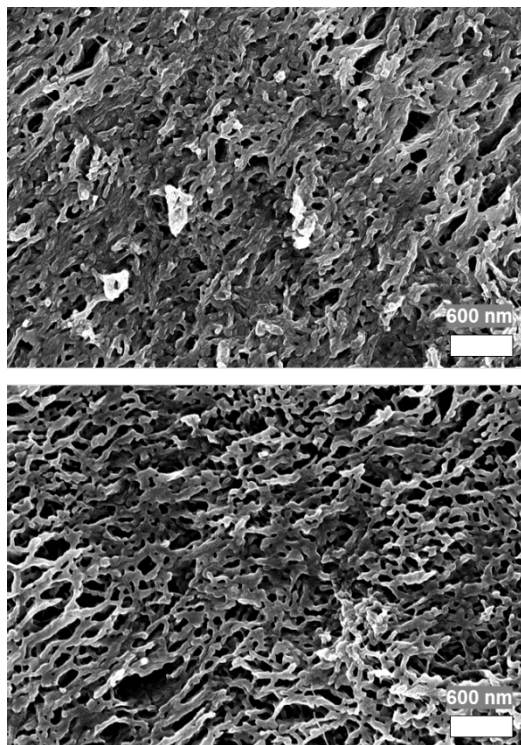


**Figure S11.** Bottom surface SEM images of images NPMs derived from solvent cast LCL [25-51-25]. Both the non-plasma-etched (top) and the plasma etched (bottom) membrane display porous surfaces. Despite PTFE evaporating dishes having a relatively low surface energy, which favors PCOE over PLA, the bottom surfaces of solvent cast membranes were porous and did not form a skin layer. However, the porosity appears to slightly increase after plasma etching, suggesting that PCOE was favored over PLA, but not as strongly as the top surface (membrane-air interface).

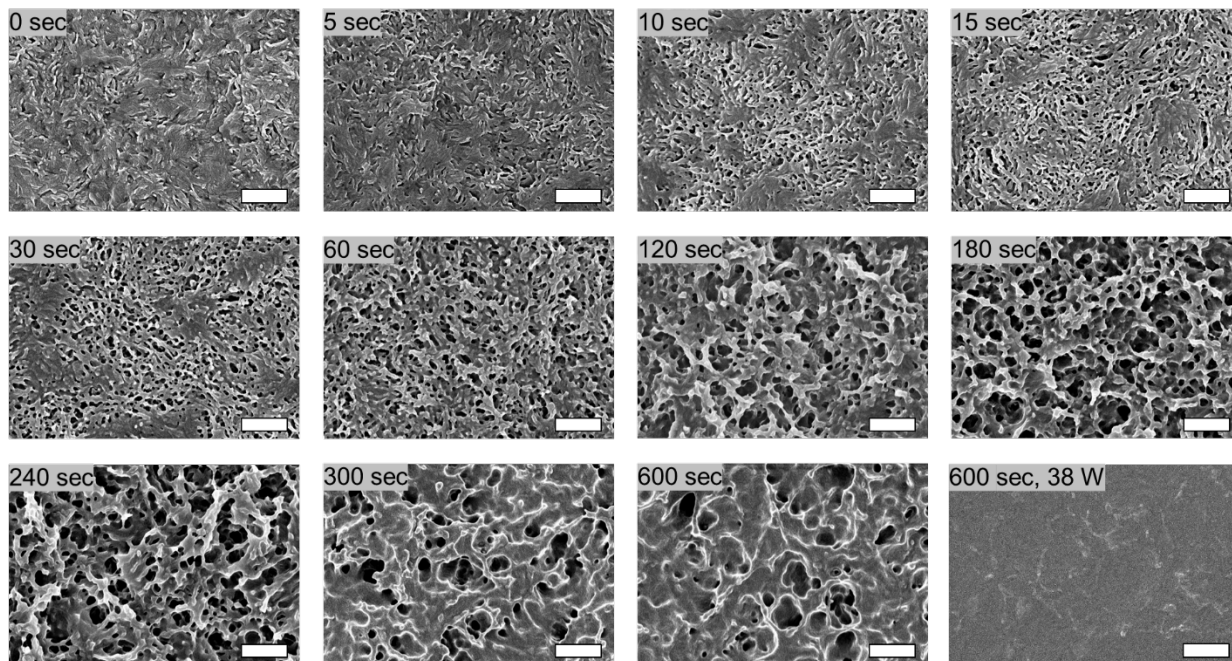


**Figure S12.** Surface SEM images of images NPMs derived from solvent cast LCL [25-51-25] under different plasma treatment exposure times. Oxygen pressure within the chamber was maintained at 0.6 bar with 30 W supplied to the RF coil, except the bottom right which was set to 38 W. Scale bars correspond to 800 nm.

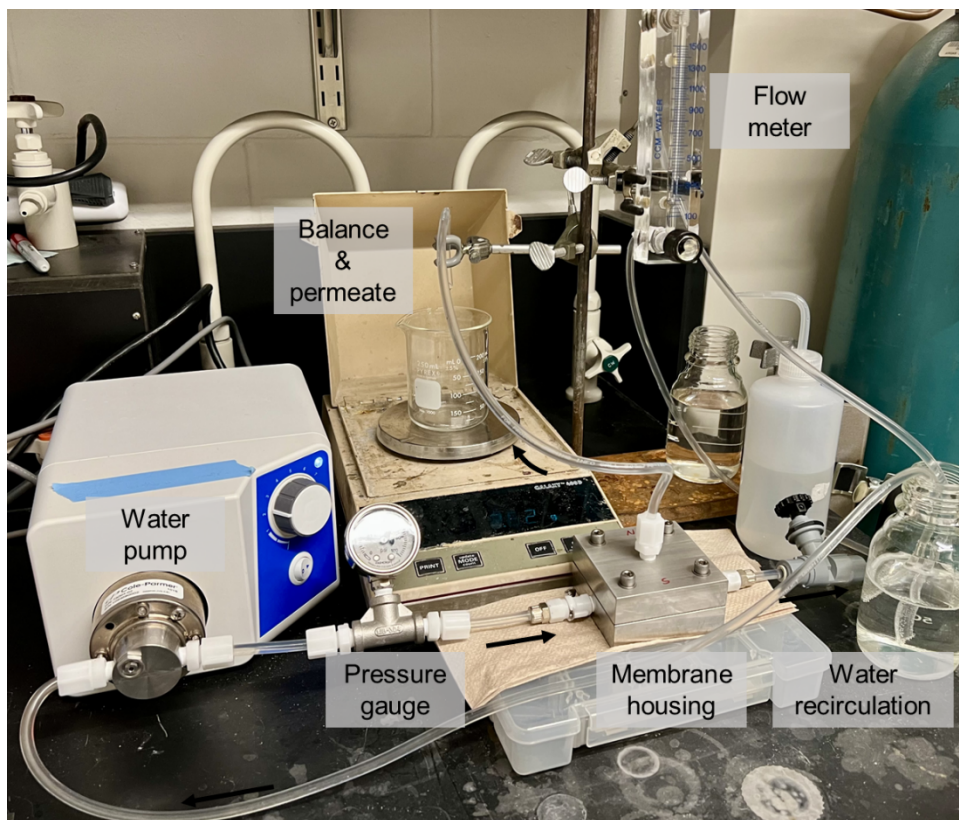


**Figure S13.** Cross-flow system used for water flux measurements. A water pump directs the flow of deionized water. A pressure gauge is placed in line between the pump and the membrane housing. Water flows (left to right) through the membrane housing (aluminum block), passes through a water flow meter, then finally recirculates through the system. Water that permeates the membrane flows upward out of the membrane housing, where it flows into a beaker on a balance. The permeate mass is tracked over time to determine the water flux.

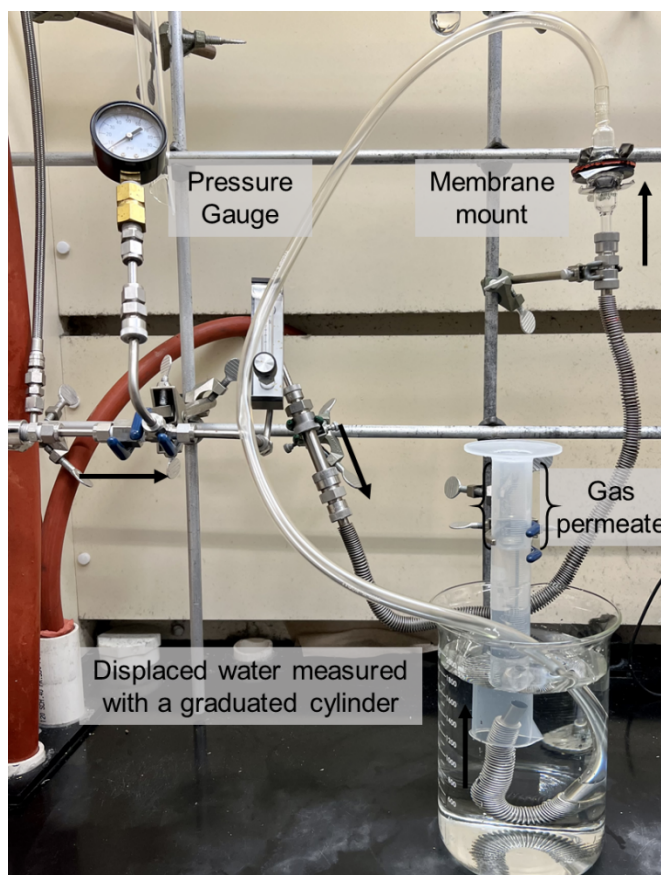


**Figure S14.** Gas permeation and water displacement apparatus used for air flux measurement. Air passes through the metal tubing from left to right, going through a pressure gauge and flow meter. The airflow is then directed to the membrane mount (top right), which consists of the nanoporous membrane sandwiched between two rubber gaskets, further sandwiched between two 15 mm diameter Schlenk adapters. After passing through the membrane, the gas is directed into a water-filled graduated cylinder inverted within a beaker of water to measure the volume of water displaced over time.

## References

---

- <sup>1</sup> Vidil, T.; Hampu, N.; Hillmyer, M. A. *ACS Cent. Sci.* **2017**, 3(10), 1114–1120.
- <sup>2</sup> Pitet, L. M.; Chamberlain, B. M.; Hauser, A. W.; Hillmyer, M. A. *Polym. Chem.* **2019**, 10(39), 5385–5395.
- <sup>3</sup> Dorgan, J. R.; Janzen, J.; Knauss, D. M.; Hait, S. B.; Limoges, B. R.; Hutchinson, M. H. J. *Polym. Sci., Part B: Polym. Phys.* **2005**, 43, 3100–3111.
- <sup>4</sup> Hillmyer, M. A., Laredo, W. R., & Grubbs, R. H. *Macromolecules*, **1995**, 28(18), 6311-6316.
- <sup>5</sup> Sample, C. S.; Kellstedt, E. A.; Hillmyer, M. A. *ACS Macro Lett.* **2022**, 11(5), 608–614.
- <sup>6</sup> Smith, B. C. *Spectroscopy*, **2018**, 33(5), 20-23.
- <sup>7</sup> Smith, B. C. *Spectroscopy*, **2018**, 33(1), 14-20.
- <sup>8</sup> Bassi, I. W.; Fagherazzi, G. *European Polymer Journal*, **1968**, 4, 123-132.
- <sup>9</sup> Natta, G.; Bassi, I. W.; Fagherazzi, G. *European Polymer Journal*, **1967**, 3, 339-352.